

Experimental studies in antisolvent crystallization: Effect of antisolvent ratio and mixing patterns

Aniket S Waval, Pooja Patel, Parag R Nemade, Channamallikarjun S Mathpati*

Department of Chemical Engineering, Institute of Chemical Technology, N. Parekh Road, Matunga 400 019, East Mumbai, India

E-mail: cs.mathpati@ictmumbai.edu.in

Received 4 March 2019; accepted 14 November 2019

The crystals size and distribution play an important role in drug properties which has a major impact on the performance e.g., stability, solubility and bioavailability. The crystal size distribution (CSD) depends on the hydrodynamics and local degree of supersaturation in the crystallizer. In this study, we have investigated the effects of various operating conditions (antisolvent ratio, power, agitator design) using different mixing techniques such as impellers and ultrasound on CSD and average crystal size (ACS). It is found that mixing plays a dominant role in CSD and ACS. The hydrofoil (axial flow impeller) provides a wide range of ACS (406 to 240 μm) at lower power as compared to Rushton turbine (radial flow impeller) (395 to 375 μm). The mixed flow impeller produces the intermediate crystal size (365 to 345 μm). The increase in the antisolvent ratio results in a decrease in ACS. The same results observed for the power input.

Keywords: Antisolvent crystallization, Agitator design, Ultrasound, Non-uniformity, Mixing patterns, Stirred tank

Crystallization is one of the oldest and widely used unit operations for many purposes, such as solid-solid separation, purification etc. Antisolvent crystallization is one of the preferred ways of crystallizing of heat sensitive materials such as APIs¹⁻³. The factors such as mixing, flow pattern, local and bulk conditions in the system such as temperature, shear, concentration etc. affect directly on the crystal size and morphology.

The crystal size distribution (CSD) is one of the major factors that must be considered to understand the success of the process. CSD is dependent on various design and operating parameters such as crystallizer type (batch, continuous or semi-batch) and geometry (stirred tank, Swenson-walker, jets etc.), selection of antisolvent (purity, composition, quantity), temperature, antisolvent addition rate, position of antisolvent addition (at surface, near high shear region etc.), mixing pattern, homogeneity, power input method (impeller, sonication, jets, etc.) in the system etc. These all factors affect CSD and ACS to a great extent.

Barette *et al.*⁴ studied the effect of hydrodynamics and mixing pattern of 39° upward pitched blade impeller. CFD study has been done to figure out antisolvent addition location to limit time scale across antisolvent addition rate. Park & Yeo⁵ studied the effects of various parameters such as the concentrations

of carbamazepine (drug) solution (ethanol), crystallization temperatures, mixing rates of the carbamazepine solution and antisolvent (water) using ultrasound. It was investigated that; the average crystal size increased when (1) process carried out at a high temperature, (2) when both streams mixed very slowly (less than 2 mL/min) and (3) when the process carried out using sonication. The average particle size decreased for higher carbamazepine concentration in solvent increased and rapid mixing of both the streams. It was concluded that ultrasound does affect only at the initial stage of crystallization and does not affect the thermal stability and crystallinity of crystals. Cogoni *et al.*⁶ studied the effect of different antisolvents with varied polarity index (ethanol, acetic acid and isopropanol) on the CSD of sodium chloride at different temperature and feed rate. It was observed that the crystal size increases by increasing the temperature or decreasing the antisolvent feed rate or using an antisolvent with a low polarity index. Bhangu *et al.*⁷ studied the effect of various ultrasonic frequencies and power on the mean crystal size, crystal size distribution, induction time, and type of polymorph of paracetamol. Ethanol as a solvent for paracetamol and water as an antisolvent was used for the experiments. It was reported that polymorphs of paracetamol forms by increasing frequency up to

98 Hz. It was also observed the reduction of average particle size and CSD. Wada *et al.*⁸ investigated the effect of antisolvents on the sodium chloride crystal size distribution by using a continuous supply of N₂ bubbles. The addition of methanol in saturated salt solution results in larger crystal size than using ethanol as antisolvent. The CSD shift to the right side for methanol used as antisolvent. Attempts have been made for the using of supercritical antisolvents. Supercritical carbon dioxide was used as antisolvent for the polymer and ethyl acetate for the micronization and co-precipitation of quercetin particles with ethyl cellulose. The same system was used for the precipitation of ethyl acetate^{9,10}.

The objective of the present study is to understand the effect of various mixing techniques, flow patterns generated by different impellers, power input and antisolvent ratio on CSD and ACS. In this study, two different aspects of crystallization were studied; A) effects of different impellers, speed, power dissipation, antisolvent ratio and flow pattern generated by the impellers and B) effect of energy input technique, antisolvent ratio, uniform & non-uniform mixing on CSD & ACS. The first part deals with the effect of flow patterns generated by different impellers at various operating conditions on the ACS and CSD. The power dissipated in the system was also correlated with the ACS. It was found that the axial flow pattern results in the narrow CSD. In the second part, the effect of local and bulk concentration differences of saturated solution and antisolvent was studied. The uniform concentration was maintained by using impeller (mild agitation) and ultrasound. The ultrasound crystallization study was done to investigate the effect of very high power input on the CSD and ACS.

Experimental Section

Sodium chloride (Common salt) of TATA chemicals was purchased from the grocery store. Antisolvent, methanol (AR grade) was purchased from SD fine chemicals Ltd., India. Distilled water has been prepared in the laboratory to make a saturated solution of sodium chloride. In all experiments, saturated solution of sodium chloride (35% NaCl and 65% distilled water) was prepared and used.

Figure 1 is showing the schematics of experimental setup for the antisolvent crystallization of sodium chloride, which used for all experiments. Minor changes were done for different studies. The setup has three necks (the schematic shows only; the one was

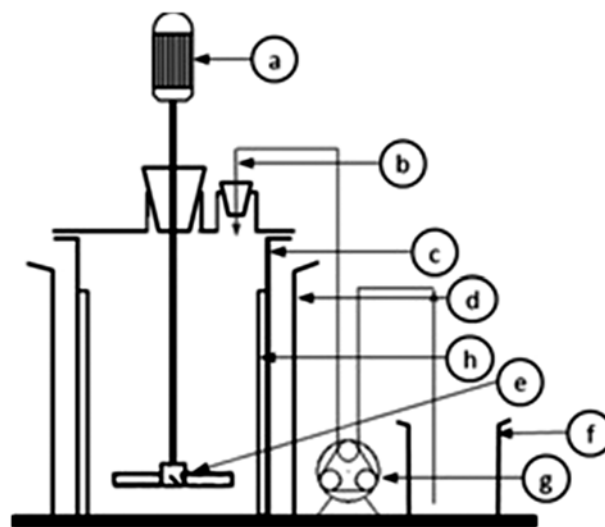
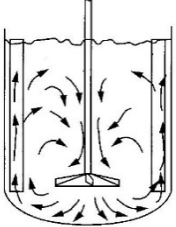
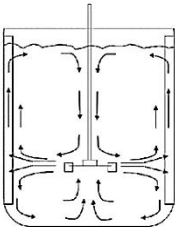
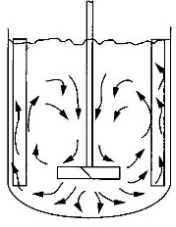


Fig. 1 — Experimental set up for antisolvent crystallization.

always kept either close during operation or open during antisolvent addition) flat bottom glass vessel of capacity 0.3 L. The glass vessel was of 0.06 m diameter and 0.1 m height was used. The liquid height in the vessel was maintained between 0.05 to 0.08 m. The clearance between the impeller and the bottom wall was kept 0.02 (± 0.002) m. Four numbers of baffles were incorporated to avoid vortex formation in the vessel. The experiments were carried out to compare three different impellers (shown in Table 1) to investigate the effect of flow pattern, ratio of antisolvent with saturated solution of sodium chloride, impeller speed and power input on CSD and ACS at 25°C (± 2). The temperature was maintained using a water bath (temperature kept between 23 to 27 °C). The antisolvent to saturated sodium chloride solution ratio was varied from 0.1 to 0.4 with a constant impeller speed (200 rpm).

The uniformity and non-uniformity experiments were performed in the same experimental setup shown in Fig.1. The 45° pitched blade impeller of 0.03 m was used for mixing in the vessel. The impeller speed was kept as low as possible, i.e. 50 (± 5) rpm; to mix both saturated solution of sodium chloride and antisolvent (methanol) coming through peristaltic pump from methanol storage beaker at defined flowrate. For non-uniformity experiments, the impeller was removed from the setup. The addition of the antisolvent was done on the surface of the saturated solution. The setup was kept as it is and no agitation or mixing was provided. The care was taken to mix the antisolvent, saturated solution and the mixture of both by convective phenomenon by density difference only.

Table 1 — Impeller details			
Impeller Design	Hydrofoil	Rushton Turbine (RT)	45° Pitched Blade Turbine (PBT)
Flow pattern			
Flow pattern	Axial flow	Radial flow	Mixed flow
Diameter (m)	0.035	0.04	0.03
Power number	0.3	5.2	2
Remarks	Less turbulence and shear, Keeps solids in suspension	Highly turbulence at impeller walls, high shear, not suitable for solid suspension.	Mixed performance, convective motion desirable for solid suspension compared to turbulence

The effect of antisolvent ratio for uniform and non-uniform on CSD and ACS was studied at 25°C (± 2).

The ultrasound experiments were performed in the bath, procured from Dakshin, Mumbai with a power range of 100–200 W and frequency of 40 kHz and 25 kHz. The ultrasound experiments were done by placing the glass vessel in the bath at power 100 to 200 W, keeping the temperature constant at 25°C (± 2). The power was kept constant (200 W) to investigate effect of different antisolvent ratios with saturated salt solution (0.1 to 0.4) on CSD at 25°C (± 2), using the same setup shown in schematics (Fig. 1). The pitched blade turbine (PBT) was used to maintain the concentration uniform and impeller speed was set to 50 rpm to avoid impeller effects.

Obtained crystals from all experiments were filtered under vacuum using filter cloth (50 microns) supported on the mesh. The same filter cloth was used for all experiments. The filtered solution (mother liquor) was circulated twice from the filter cloth. The filtered crystals were then dried in the oven at 100°C for 3 h. Dried crystals were analyzed for crystal size distribution and average particle size. Obtained crystal images were captured by using Moticam 1000 camera mounted on a Leica Galen III microscope; a 4X objective lens with 10X zoom was used for 40X magnification. Further, the size was determined by WebPlotDigitizer and in-house developed MATLAB code.

Result and Discussion

Effect of different agitators on crystallization

The effect of mixing and agitation on the crystallization process is widely studied¹¹⁻¹³. In this work, we studied the effect of the ratio of antisolvent to a saturated salt solution, impeller type, speed and power input on the CSD and ACS.

Effect of antisolvent ratio on particle size

The liquid circulation rate and flow pattern both depend on the type of impeller. In this study, the effect of the ratio of antisolvent with the saturated solution and impeller type (based on the flow pattern generated) was studied. It was observed for all type impellers that, as the antisolvent ratio increase, the ACS decreases; the higher effect was observed for RT (435 to 300 μm) and hydrofoil (406 to 240 μm) as impellers affects the mixing pattern in the vessel (Fig. 2a). The intermediate average crystal size was observed for PBT (400 to 260 μm), which generates a mixed flow pattern.

The local concentration of the antisolvent and saturated solution affects nuclei and crystal growth. Hydrofoil showed minimum crystal size at the same antisolvent ratio as compared to the pitched blade and Rushton type impeller. Flow patterns generated by impellers used in this study were shown in Table 1. The flow pattern developed by hydrofoil is radial which develops circulation loops in the vessel, from the top surface to the bottom of the vessel. The length of circulation loops generated by hydrofoil is longer

than the same generated by PBT and RT, as both impellers generate mixed and axial flow patterns, respectively. The circulating flow pattern created by hydrofoil continuously renews the surface of saturated solution which reduces the difference between local and bulk concentration when antisolvent touches the saturated solution. The nuclei continuously generate at the surface and further mix and circulate in the system which allows uniform growth of maximum nuclei. This results in an increased number of nuclei and uniform growth of the crystals with uniform CSD.

Effect of impeller speed on particle size

The increase in the impeller speed tends to uniform concentration, which results in steady growth as the level of supersaturation in these areas observed to be constant¹⁴. The variation in impeller speed results in the varied circulation velocity and power requirement which eventually alters the flow pattern inside the vessel. The impellers selected in this study such as each, generates a different flow pattern. The effect of impeller speed on the ACS is reported in Fig. 2b. It was observed that as the speed of impellers increases the ACS decreases. The ACS obtained by RT (395 μm) at 100 rpm was the largest average size and smaller range (395 to 375 μm at 100 and 250 rpm respectively) of ACS was obtained by the other two impellers. PBT has shown a wide range of particle size range (385 to 345 μm at 100 to 250 rpm respectively) for RT and hydrofoil. Hydrofoil showed the least average particle size range (365 to 345 μm) impeller speed between 100 to 250 rpm than RT. The average particle size is dependent on the number of nuclei generated and their growth which can be controlled by the mixing of saturated solution and antisolvent in the system.

The rotational speed of an impeller plays an essential role in circulation velocity and flow patterns. The pitched blade develops a mixed flow pattern that circulates fluid in axial as well as radial direction. As the rotational speed of the PB increases, the circulation velocity increases hence the mixing which results in uniformity in concentration. During antisolvent addition, as soon as antisolvent touches the surface of the saturated solution the nuclei generates. A flow pattern generated by PB and hydrofoil allows the renewal of surface which results in the mixing of nuclei generated at or near the surface during antisolvent addition throughout the system. The PBT possesses both flow patterns, axial and radial. At lower speed, flow is more radial and as

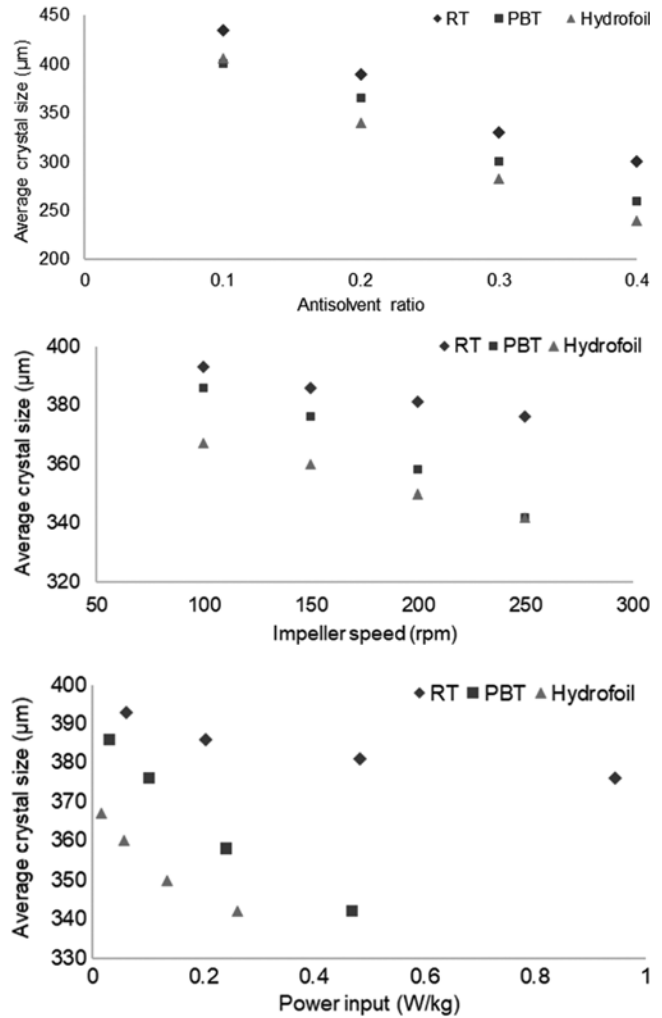


Fig. 2 — (2a) Effect of antisolvent ratio on ACS for different impellers at constant impeller speed (200 rpm); (2b) Effect of the impeller type and impeller speed on ACS at constant antisolvent to saturated solution ratio (antisolvent ratio= 0.2); (2c) Effect of power input on the ACS with various impellers at constant antisolvent ratio i.e. 0.2.

the speed increase, the flow becomes more axial. It has been observed that the PBT has covered the ACS obtained for RT and hydrofoil. The ACS (385 μm) obtained at a lower speed (100 rpm) for PBT was observed to be the same as ACS obtained while using RT (395μm at 100 rpm). The same-sized ACS (345 μm) was obtained for PBT and hydrofoil at 250 rpm.

Effect of power input on particle size

The effect of power input per unit mass (m) has been correlated with the power input by impellers shown in Fig. 2c. The power input is a function of impeller speed (N), diameter (D) and power number (N_p) at the specific diameter and calculated by using

$$P (tn W) = N_p \rho N^3 D^5 \quad \dots (1)$$

The RT has power number higher than the PBT and hydrofoil, whereas hydrofoil has the lowest power number than RT and PBT (shown in Table 1). The variation in power number and diameter results in the drastic change in power requirements at the same speed. Figure 2c shows the effect of power input by different impellers on ACS. The RT showed a narrow ACS range (395 to 375 μm) at higher power input per unit mass (0.85 to 13.5 W/kg) and hydrofoil showed a broad range of ACS (365 to 345 μm) at lower power input (0.24 to 3.8 W/kg). The PB showed an intermediate ACS range (385 to 345 μm) at intermediate power input (0.4 to 6.7 W/kg). The Rushton turbine develops radial flow which increases the drag on the impeller blades which results in the higher power number at lower rotating speed as compared to the hydrofoil and pitched blade impeller. Only the radial flow pattern generated by RT results in poor mixing leads to the narrow size range at higher power input. PB and hydrofoil showed intermediate and broad size distribution at lower power input as compared to RT.

To obtain defined crystal size at optimized power input, we need to select appropriate operating and design parameters such as antisolvent ration, impeller type based on flow pattern generated, impeller speed and power input.

Effect of impeller on CSD

The antisolvent ratio and impeller speed alter ACS at varied conditions. The effect of these conditions on CSD for different impellers shown in Fig. 3. To understand the effect of flow pattern generated by impellers on CSD has been studied at constant impeller speed (200 rpm) and antisolvent to saturated solution ratio (0.4:1). The curve RT (in Fig. 3) showing broad CSD for RT. The RT develops a radial mixing pattern which results in two mixing zones (above impeller and below impeller). The material or liquid circulates and mixes in above and below impeller zones independently. The material from both zones mix near the vessel wall where the radial flow is negligible. The difference in bulk and local concentration increases due to the mixing in separated zones. The antisolvent was added to the stirred tank on the surface. At this point (antisolvent addition point i.e., on the surface) mixing was observed to be poor due to low circulation and lower intensity of mixing. The non-uniformity in mixing resulted in the broader range of crystal size. The irregular mixing

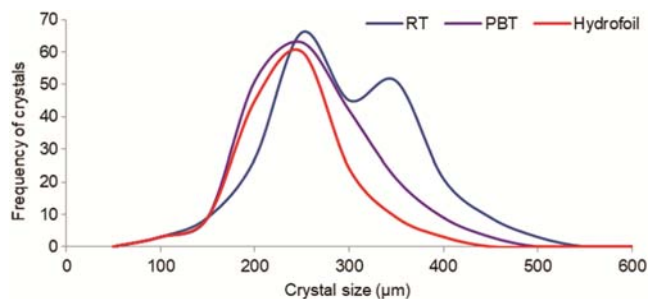


Fig. 3 — CSD for various impellers at constant impeller speed and antisolvent to saturated solution ratio (impeller speed= 200 rpm & antisolvent ratio= 0.4).

pattern results in agglomeration of crystals and high shear at impeller results in the breakup of agglomerated crystals, results in two maxima in curve RT (Fig. 3). The hydrofoil impeller generates an axial flow pattern which recirculates the liquid throughout the vessel. Which reduces the bulk and local concentration and generates nuclei throughout the vessel. The crystal growth is more uniform for Hydrofoil than that of RT as the liquid is uniformly circulated in the vessel eventually results in narrowed CSD. The intermediate CSD obtained for PB due to the mixed flow pattern. The PB generates both axial as well as radial flow; this results in two zones and intermixing mixing of these two zones same as RT and PB respectively. This mixed flow pattern generates lower crystals higher than hydrofoil and larger crystals smaller than RT. The intermediate behavior of CSD observed for PB.

Effect of uniformity and energy mode

Effect of non-uniformity and antisolvent quantity

The non-uniformity in the vessel results in a difference degree of supersaturation in the system. In the case of antisolvent crystallization, the non-uniformity due to the improper mixing of the methanol (antisolvent) and saturated solution. Nuclei forms at the contact zone between methanol and saturated solution. The rate of the nucleation depends on the degree of local supersaturation, which in turn depends on the local concentration of the salt in solution and on the rate of generation of salt crystals. The prolonged contact time results in the thicker zone of NaCl crystals. Since the diffusion of the solute controls this zone, the rate of crystal generation becomes slower. The non-uniform nucleation rate decreases which favors the growth of the nuclei that already present in the system¹⁵. As soon as the antisolvent comes in contact with the saturated solution, nuclei form on the surface. The saturated

solution surface gets saturated with the antisolvent; the only difference in the densities results in the circulation and mixing. Due to the uncontrolled circulations and concentration, different nuclei grow at different rates and irregularities observed at faces; this can be seen from the SEM image shown in Fig. 4. The unmixed system results in the variation in nuclei growth, which can also be seen by more than one maxima or longer tail, shown in Fig. 5a.

The effect of the ratio of antisolvent to the saturated solution on the CSD was studied, which is shown in Fig. 5a. It can be seen from the figure that the ACS decreases as the antisolvent amount increases. The continuous addition of the antisolvent results in the increased number of nuclei and circulation rate due to continual change in densities. The amount of antisolvent alters the number of nuclei produced, density, circulations for mixing and growth of the crystal.

Effect of uniformity on crystallization

The effect of antisolvent to saturated solution ratio on ACS and CSD has been studied at constant antisolvent flowrate. The study also involves the effect of energy mode input on the CSD and ACS. The CSD narrowed due to the well-mixed behavior of the system (Fig. 5b) as compared to the non-uniform system (Fig. 5a).

We can also conclude from Fig. 5a and 5b that the CSD obtained at different mixing conditions may vary, but the size of the crystals obtained in both systems is the same size range. The mixing and concentration uniformity only affect the CSD not the size of crystals.

Effect of ultrasonication on crystallization

Ruecroft *et al.*¹⁰ studied the effects of antisolvent ratio and uniformity on the ACS and CSD. Further

crystallization study was done to understand the effect of ultrasound power and antisolvent ratio on the same at constant antisolvent flowrate and constant power input respectively. Ultrasound causes the primary nucleation in a saturated solution; therefore, crystals size reduces even at low antisolvent quantity. The heat generated at the molecular level due to the collision of vapour cavity bubbles which results in the evaporation of solvent, causes sudden cooling and increases the supersaturation. The supersaturation generates nuclei at a micro level further this nucleus grows as crystals^{16, 17}. The ultrasonication reduces

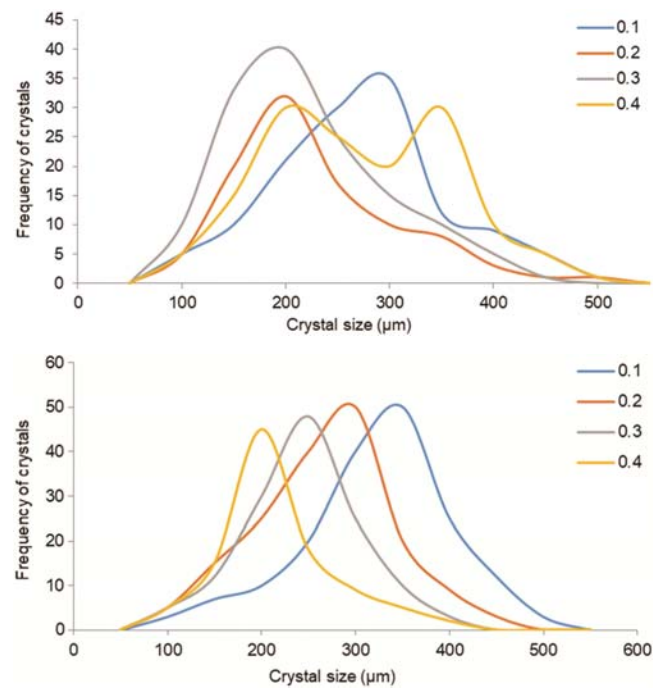


Fig. 5 — (5a) CSD obtained at different antisolvent ratios without using any impeller system; (5b) CSD obtained at different antisolvent ratios under stirring (impeller speed= 50 rpm).

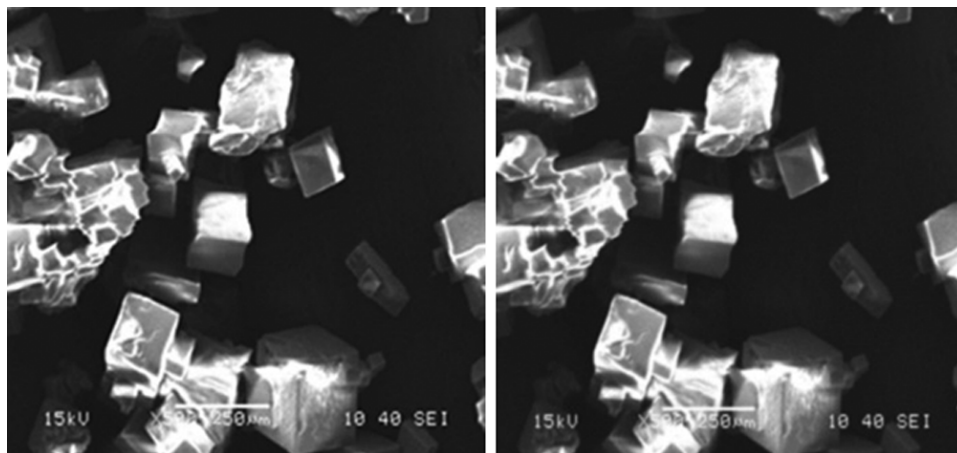


Fig. 4 — SEM images of NaCl crystals showing randomness in size and growth at different faces.

the size reduction and separation operation which minimizes the energy¹⁸. Lee *et al.*¹⁵ observed the symmetric cubic structure of NaCl crystal obtained from ultrasound crystallization. Crystals obtained from ultrasound crystallization shown uniformity in shape and size as compared to the same obtained from the well-mixed system.

Effect of power input on crystallization

Park & Yeo⁵ observed for carbamazepine that the crystal size decreases as the ultrasonic power input increases. Li-Yun *et al.*¹⁹ found that the hydroxyapatite particles formed above 300 W input power, below this power particle formation, are not possible. The crystal size decreased as the power input increases. An increase in power input results in increases in the turbulence due to which molecules collide on each other. The collision enhances the penetration through stagnant film and gets into the crystal lattice uniformly and quickly. In this study, the effect of power input (at a constant temperature of 25°C) and the antisolvent ratio on the average crystal size was studied. Uniform crystal size was achieved by ultrasonication. The high degree of mixing in the system attained due to microscale mixing. The increase in power dissipation increases the degree of micromixing which creates more nuclei available for crystal growth; this leads to uniform and smaller particle size. The average crystal size and distribution are also strong functions of power input which is shown in Table 2 and Fig. 6a. It was also observed that distribution narrowed when power input increases above 150 W. From the results shown in Fig. 6a, we can conclude that the ACS is closely following a linear relationship with power for ultrasonic crystallization.

Effect of the antisolvent ratio on crystallization

Park & Yeo⁵ and Borissova *et al.*²⁰ studied the effects of the antisolvent addition rate on the crystallization were studied. In the current study, the effect of the antisolvent ratio on the crystal size distribution was studied at constant energy input (200 W). Figure 6b shows that, as the ratio of antisolvent increases from 0.1 to 0.4, the ACS

decreases from 320 to 220 μm along with a narrowing of the CSD curve.

Comparison of ACS obtained at different conditions

The effect of uniformity, non-uniformity and power input mode was studied at varied antisolvent to saturated solution ratio (shown in Fig. 7). The non-uniformity in the system results in the larger crystal size as compared to the well-mixed system and ultrasonication. The trend follows the same for all conditions; either system is non-uniformly or uniformly mixed. The effect of power input can be seen in Fig. 5b, as the power input increases the average crystal size decreases. High power dissipation and degree of uniformity were observed in case of ultrasound-assisted crystallization than mechanically stirred or unmixed system. The high power input and uniform concentration in the system result in the smaller crystal size. The smaller size of crystals may also occur due to the breakage of particles at energy input. It was also observed that as the antisolvent addition rate increase, the average crystal size decreases, obtained under different energy input modes. The increase in the antisolvent quantity

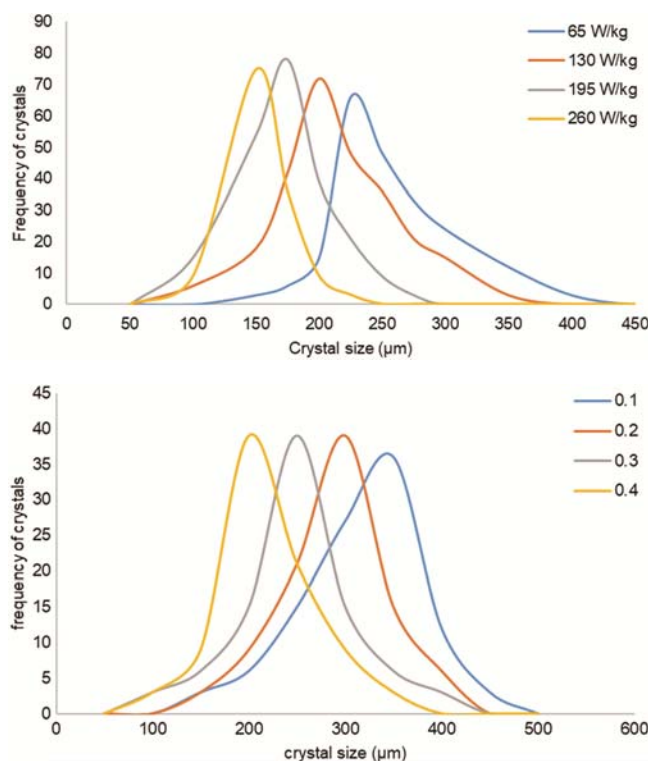


Fig. 6 — (6a) Crystal size distribution at different power input per unit mass at the constant antisolvent ratio i.e. 0.2 using ultrasound energy; (6b) Particle size obtained at the different anti-solvent ratio with saturated solution and constant power input by sonication.

Table 2 — Average crystal size obtained at various power input

Power input (W/kg)	Average crystal size (μm)
65	253
130	215
195	177
260	159

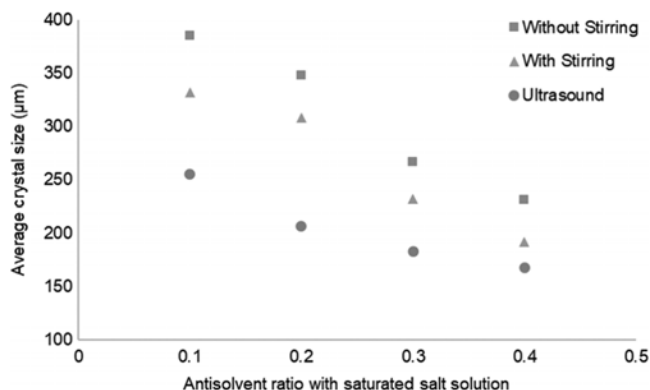


Fig. 7 — Effect of anti-solvent ratio and power input mode on crystal size.

increases the number of nuclei in the system for all conditions, which results in a decrease in the size of crystals obtained at all conditions including non-homogeneous systems.

Conclusion

The antisolvent crystallization was studied for methanol (antisolvent) and saturated sodium chloride solution at various conditions and compared with each other. Effect of uniformity and non-uniformity (concentration gradient of antisolvent and saturated solution mixture), antisolvent to saturated solution ratio, ultrasound power on the crystal size distribution and ACS was studied. It was observed that unmixed or non-uniform conditions during mixing results in uneven and uncontrolled growth of the crystals. The crystallization using ultrasound produces a smaller size of crystals as compared to the other techniques. Crystal size distribution was shifted towards smaller crystal size as power increases. The distribution narrows at higher power (>150 W). The study of the effect of flow patterns on the crystallization process was studied. To generate different flow patterns three different impellers were used. In this study, it was observed that the ACS affects significantly by the flow pattern. The axial flow circulates the liquid throughout the vessel and results in the uniform mixing in above and below the impeller. The radial flow impeller produces larger size particles as compared to axial and mixed flow impellers. The mixed flow impeller which possesses both flow

patterns, shown the intermediate average crystal size. The power and impeller rotational speed are inversely proportional to the ACS. The desired ACS can be obtained by selection of proper impeller type, impeller speed, power input and antisolvent ratio.

Acknowledgement

The authors would like to acknowledge the Science & Engineering Research Board (SERB) (File No: EMR/2016/001563) for the fellowship and financial support.

References

- 1 Fernández-Ponce M T, Masmoudi Y, Djerafi R, Casas L, Mantell C, Ossa E M D L & Badens E, *J Supercrit Fluids*, 105 (2017) 119.
- 2 Gu T, Yeap E W Q, Cao Z, Ng D Z L, Ren Y, Chen R, Khan S A & Hatton T A, *Adv Healthc Mater*, 7 (2018) 1.
- 3 Lonare A A & Patel S R, *Int J Chem Eng Appl*, 321 (2013) 337.
- 4 Barrett M, O'Grady D, Casey E & Glennon B, *Chem Eng Sci*, 66 (2011) 2523.
- 5 Park M -W & Yeo S -D, *Chem Eng Res Des*, 90 (2012) 2202.
- 6 Cogoni G, Baratti R & Romagnoli J A, *Ind Eng Chem Res*, 52 (2013) 9612.
- 7 Bhangu S, Ashokkumar M & Lee J, *Cryst Growth Des*, 16 (2016) 1934.
- 8 Wada Y, Matsumoto M & Onoe K, *J Cryst Growth*, 448 (2016) 76.
- 9 Djerafi R, Masmoudi Y, Crampon C, Meniai A & Badens E, *J Supercrit Fluids*, 105 (2017) 92.
- 10 Ruecroft G, Hipkiss D, Ly T, Maxted N & Cains P W, *Org Process Res Dev*, 9 (2005) 923.
- 11 Abbasi E & Alamdari A, *J Chem Eng Jpn*, 408 (2007) 636.
- 12 Akrap M, Kuzmanic N & Prlic-Kardum J, *Cryst Growth*, 312 (2010) 3603
- 13 Rane C V, Ekambara K, Joshi J B & Ramkrishna D, *AIChE J*, 60 (2014) 3596.
- 14 Wantha W & Flood A E, *Chem Eng Commun*, 195 (2008) 1345.
- 15 Lee J, Ashokkumar M & Kentish S E, *Ultrason Sonochem*, 21 (2014) 60.
- 16 Bučar D -K & MacGillivray L R, *J Am Chem Soc*, 129 (2007) 32.
- 17 Gracin S, Uusi-Penttilä M & Rasmuson Å C, *Cryst Growth Des*, 5 (2005) 1787.
- 18 Ramisetty K A, Pandit A B and Gogate P R, *Ind Eng Chem Res*, 52 (2013) 17573.
- 19 Li-yun C, Chuan-bo Z & Jian-feng H, *Mater Lett*, 59 (2005) 1902.
- 20 Borissova A, Dashova Z, Lai X & Roberts K J, *Cryst Growth Des*, 4 (2004) 1053.